

Abstract

We argue that in the quarter-filled ladder compound NaV_2O_5 the quasi-one-dimensional spin system is strongly coupled to a low-energy antiferroelectric mode of the excitonic type. This mode results from the interplay between the electron hopping along the rungs of the vanadium two-leg ladders and the Coulomb repulsion between electrons. The charge ordering observed in sodium vanadate at $T_c = 34\text{K}$ corresponds to the softening of the antiferroelectric mode. We consider the spin-isospin model, which describes the spin and low-energy charge degrees of freedom in sodium vanadate. Within this model we explain the observed anomalous temperature-dependence of the dielectric susceptibility at T_c and the midinfrared absorption continuum. We identify the broad structure in the low-energy optical absorption spectrum of NaV_2O_5 with the continuum formed by two spinons and one low-energy charge excitation.

Spin-isospin model of NaV_2O_5

M. V. Mostovoy, J. Knoester, and D. I. Khomskii

*Theoretical Physics Institute and Materials Science Center,
University of Groningen, Nijenborgh 4,
9747 AG Groningen, The Netherlands*

April 26, 2024

1 Introduction

Sodium vanadate (NaV_2O_5), first studied in the seventies [1], has become an object of intensive experimental and theoretical investigations after the discovery of the phase transition at $T_c = 34\text{K}$ [2]. Several physical concepts, such as bipolarons [4], spin-Peierls transition [2, 3], and charge ordering [5, 6, 7], have been proposed to explain the properties of this material. Yet, despite all the efforts, the low-temperature crystal structure of sodium vanadate remains controversial and the nature of the low-energy excitations in this material is still poorly understood.

In α' - NaV_2O_5 the vanadium ions form two-leg ladders organized in layers (see Fig. 1). Until recently it was assumed that the vanadium ladders with one electron per rung are equivalent to spin- $\frac{1}{2}$ chains, so that sodium vanadate is a quasi-one-dimensional spin system. Indeed, this material is a good insulator and its magnetic susceptibility has temperature behavior similar to that of the Heisenberg spin- $\frac{1}{2}$ chain with the exchange constant $J \sim 560\text{K}$ [8]. At $T_c = 34\text{K}$ sodium vanadate undergoes a phase transition into a state with a spin gap. Below T_c the lattice period along the ladders (b -direction) and perpendicular to ladders within the layers (a -direction) doubles, while the period in the direction perpendicular to the layers (c -direction) increases by a factor of four [3]. The transition was initially interpreted as a spin-Peierls transition, driven by the instability of spin- $\frac{1}{2}$ chains against the formation of local dimers.

However, more recent experimental studies of NaV_2O_5 revealed some inconsistencies in that interpretation. First, sodium vanadate does not show the strong suppression of T_c by magnetic field, characteristic for spin-Peierls systems [9, 10]. Second, the entropy released at the transition is considerably higher than the expected release of the spin entropy [8, 9, 10]. Third, the dielectric susceptibility, measured by microwave absorption, has an anomaly at the transition temperature, which was not observed in the inorganic spin-Peierls material CuGeO_3 [11].

Recent X-ray [14, 15, 16], as well as NMR measurements [5], show that above T_c all vanadium ions are equivalent ($\text{V}^{4.5+}$), whereas below T_c , a charge disproportionation occurs. There is, however, still a controversy about the number of distinct V sites and their arrangement in the low-temperature phase [5, 17, 18, 19].

It was then suggested that the driving force of this transition is the charge ordering of electrons in the quarter-filled vanadium ladders and that the spin-

gap opens due to alternation of the spin-exchange constants, resulting from the charge ordering [6, 7]. Since sodium vanadate is an insulator both above and below T_c , the charge ordering in this material does not originate from the Fermi surface instability, as in charge-density-wave materials. Therefore in Ref. [7] we proposed a spin-isospin model, in which the rungs of the vanadium ladders are assumed to be predominantly occupied by one electron. The isospins describe the low-energy charge degrees of freedom, which in sodium vanadate are electric dipoles located on the rungs of the vanadium ladders. The isospin Hamiltonian (Ising model in a transverse field) is identical to the Hamiltonian used to describe (anti)ferroelectric transitions [20]. Below T_c the dipoles become ordered. Their directions alternate along the ladders [6, 7], which corresponding to a zigzag ordering of charges. The antiferroelectric nature of charge displacements in the vanadium-oxygen layers was confirmed by the observation of anomalies in the dielectric susceptibility close to T_c [11, 12, 13]. In Ref. [7] we showed that the antiferroelectric ordering in the system of vanadium ladders opens a spin gap.

We recall that, depending on whether the variable associated with the dipole moment of a unit cell is quantum or classical, there are two limiting types of (anti)ferroelectric transitions: a displacive transition and an order-disorder transition [20]. If the tunneling between the two states with different orientations of the dipole moment can be neglected, the transition is of the order-disorder type, described by a classical Ising model. If, on the other hand, the hopping between the two states is non-negligible, the transition is described by the quantum Ising model in a transverse field. The quantum dynamics of the electric dipoles gives rise to a branch of excitations that correspond to dipole flips propagating from one unit cell to another. At the transition temperature these excitations become gapless. The softening of the isospin excitation occurs at the wave vector of the superlattice structure appearing in the ordered phase.

In sodium vanadate the amplitude of the electron hopping along the rungs of the vanadium ladders, which plays the role of the tunneling amplitude between two states of the electric dipole, is of the same order as the Coulomb interaction between electrons on neighboring rungs (1eV) that is responsible for the charge ordering. Thus the dynamics of the antiferroelectric mode in sodium vanadate is essentially quantum and, at least close to the transition temperature, there should be low-energy charge excitations in this material.

For the antiferroelectric ordering (see Sec. 3) the soft mode has a nonzero wave vector and, therefore, cannot be directly excited in optical absorption

and Raman scattering above the transition temperature. Nevertheless, we show in this paper that the optical data do provide an evidence for the presence of the low-energy charge excitations in sodium vanadate.

The optical spectrum of sodium vanadate contains the broad absorption band covering almost the whole midinfrared region of frequencies [21, 22]. A broad peak was observed also in Raman experiments [22, 23, 24]. It was suggested in Ref. [21], that the low-energy absorption is due to the photoexcitation of the two-spinon continuum. However, to convert a photon into a pair of spinons, the presence of a permanent electric dipole moment is required (both above and below T_c , since the continuum is observed at all temperatures). This would be possible if sodium vanadate would have the ferroelectric chain-like structure that was originally proposed for this material [1], but which later was found to be inconsistent with X-ray data [14, 15, 16].

In this paper we interpret the broad peak in the low-frequency optical absorption spectrum as a three-particle continuum: two spinons plus the low-energy antiferroelectric excitation. Our mechanism crucially depends both on the presence of the soft mode, associated with the charge ordering, and on the coupling of this mode to the spin excitations.

This coupling naturally arises in the spin-isospin model discussed in Sec. 2. In Sec. 3 we consider the charge ordering in this model, which, as was already mentioned, is related to the softening of the isospin excitations discussed in Sec. 4. In Sec. 5 we apply our model to explain the anomaly of the dielectric susceptibility at T_c , while in Sec. 6 we show how the coupling between spin and isospin excitations gives rise to the low-energy optical absorption. We discuss our results in the concluding Sec. 7.

2 Spin-isospin model

The experimental observations mentioned in Sec. 1 indicate that the low-temperature properties of sodium vanadate cannot be described by only considering the spin and lattice dynamics, but that it is necessary to include also the charge degrees of freedom. On the other hand, sodium vanadate is known to be a good insulator, both above and below T_c . We, therefore, argued in [7] that the relevant electronic excitations in this material are excitons. In this section we briefly discuss the “spin-isospin” model, introduced in Ref.[7], which describes the low-energy excitations in sodium vanadate.

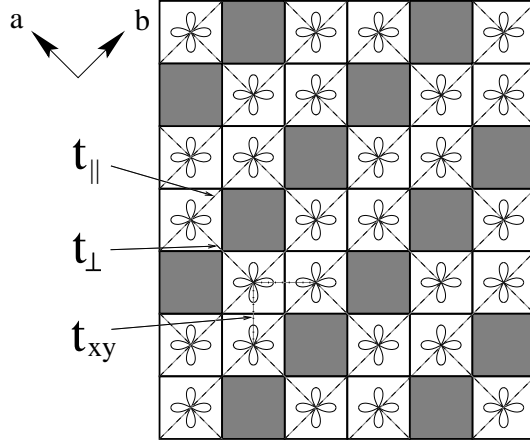


Figure 1: The crystal structure of the V-O plane in NaV_2O_5 : oxygens are located at the corners of the plaquettes, while V ions are located at their centers; the shaded plaquettes are vacant. Also shown are the vanadium ladders (dashed lines) and the relevant d_{xy} -orbitals of the V ions.

In that model we restrict ourselves to the states with only one electron per rung of the vanadium ladder. This was first suggested by Smolinski *et al.* on the basis of LDA calculations [16], which show that the electron hopping amplitude along rungs, t_{\perp} , is significantly higher than the amplitudes of hopping between the sites of different rungs (of which the largest is the hopping amplitude along ladders, t_{\parallel}). If one first neglects the interrung hopping and the interrung electron-electron interactions, then on each rung of the quarter-filled vanadium ladder there is one electron occupying the symmetric bonding state with energy $-t_{\perp}$. Due to the large value of the on-site Coulomb repulsion (which we assume to be infinite), an electron can hop only to an empty site of a neighboring rung. Then the hopping to a neighboring rung results in an energy increase $2t_{\perp}$. Thus, the quarter-filled two-leg ladder becomes equivalent to the half-filled Hubbard chain with an effective “on-rung” repulsion $U_r = 2t_{\perp}$.

This explains, in principle, why vanadium ladders are insulating. However, for the values of the hopping amplitudes, obtained in [16], $t_{\perp} = 0.38\text{eV}$ and $t_{\parallel} = 0.17\text{eV}$, the width of the one-dimensional band, $4t_{\parallel}$, is comparable with U_r . Thus the charge fluctuations on the ladder rungs are not small and the treatment of the vanadium ladder as a spin chain, as it was done in [16], is not well-justified.

The situation improves if we take into account the Coulomb interactions

between electrons on different rungs. The latter lead to an increase of the value of the “on-rung” repulsion. For instance, if we include the repulsion between the nearest-neighbor sites in ladders, V , then $U_r \approx 2t_\perp + \frac{V}{2}$, for small V . In general, the interrung Coulomb interactions make U_r not a well-defined quantity, as it becomes dependent on the positions of many electrons.

Thus, on the one hand, the interrung Coulomb interactions help to justify the assumption of one electron per rung. On the other hand, they strongly mix the symmetric and antisymmetric states on each rung, as the typical value of such interactions is of the same order as the energy separation between these two states, $2t_\perp \approx 0.75\text{eV}$. Thus, the electron position on a rung becomes an important additional degree of freedom, which makes the vanadium ladder different from a spin chain.

The two states, $u_{\mathbf{n}}$ and $d_{\mathbf{n}}$, corresponding to the two possible positions of a single electron on the rung \mathbf{n} , can be described as the up and down eigenstates of an isospin- $\frac{1}{2}$ operator, $T_{\mathbf{n}}^z$. With two spin projections there are in total four different states of an electron on a rung (see Fig. 2). The spin $\mathbf{S}_{\mathbf{n}}$ and the isospin $\mathbf{T}_{\mathbf{n}}$ are defined on the lattice, the sites of which correspond to the rungs of vanadium ladders (see Fig. 3). In this paper we ignore the three-dimensional structure of sodium vanadate and only consider one oxygen-vanadium layer. Then the lattice of our model is triangular. Furthermore, for our considerations it will not be important that in each layer the orientations of pyramids in the nearest-neighbor ladders are opposite to each other (which is why the unit cell above T_c contains two ladders). Therefore, we chose $\mathbf{f}_1 = \mathbf{b}$ and $\mathbf{f}_2 = \frac{1}{2}(\mathbf{a} + \mathbf{b})$ as the basis of the unit cell in the high-temperature phase.

The charge part of the Hamiltonian of the model, which only includes the isospin operators, has the form:

$$H_T = -2t_\perp \sum_{\mathbf{n}} T_{\mathbf{n}}^x + \frac{1}{2} \sum_{\mathbf{nm}} V_{\mathbf{nm}} T_{\mathbf{n}}^z T_{\mathbf{m}}^z, \quad (1)$$

where t_\perp is the amplitude of electron hopping along the ladder rungs and the second term describes the Coulomb repulsion between electrons on different rungs. The amplitudes $V_{\mathbf{nm}}$ are defined by

$$V_{\mathbf{nm}} = V(u_{\mathbf{n}}, u_{\mathbf{m}}) + V(d_{\mathbf{n}}, d_{\mathbf{m}}) - V(u_{\mathbf{n}}, d_{\mathbf{m}}) - V(d_{\mathbf{n}}, u_{\mathbf{m}}), \quad (2)$$

where, *e.g.*, $V(u_{\mathbf{n}}, d_{\mathbf{m}})$ is the energy of the Coulomb interaction between an electron on rung \mathbf{n} in the up state and an electron on rung \mathbf{m} in the down

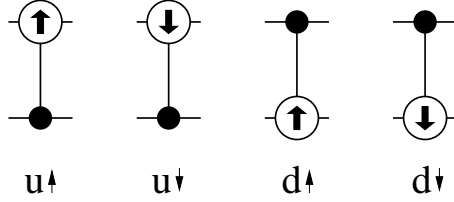


Figure 2: The four different states of a single electron on a rung represented as the eigenstates of the spin $S = \frac{1}{2}$ and the isospin $T = \frac{1}{2}$ operators.

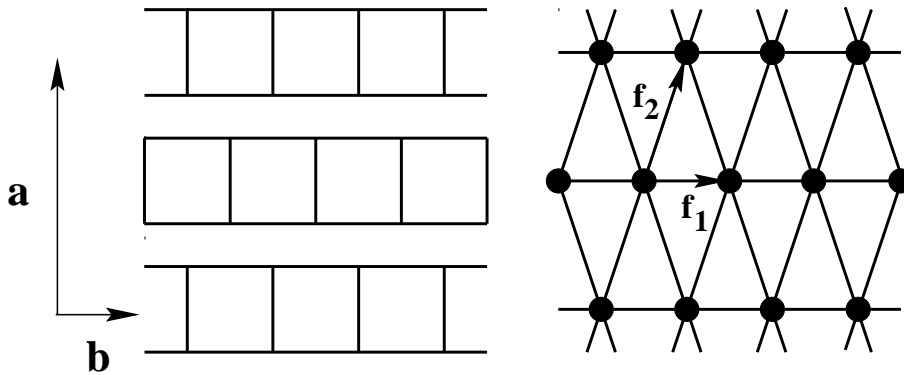


Figure 3: From vanadium ladders (left-hand side of the picture) to the effective lattice (right-hand side of the picture). The sites of the latter should be identified with the centers of the rungs of the V ladders.

state. The Coulomb interactions favor a certain charge ordering, which in our model corresponds to an ordering of the z -projections of the isospins, while the electron hopping counteracts the ordering. Since the hopping term does not commute with the Coulomb term, the isospins are quantum (rather than classical) degrees of freedom, like the orbital degrees of freedom in Mott insulators with orbital degeneracy [25].

We now turn to the spin contributions to the Hamiltonian. The spin exchange results from virtual hopping of electrons between neighboring rungs, and the exchange interaction is the strongest in the ladder direction. For the half-filled Hubbard chain the exchange interactions between spins on two neighboring sites has the form $\frac{2t^2}{U}S_{12}$, where $S_{12} = 2(\mathbf{S}_1 \cdot \mathbf{S}_2) + \frac{1}{2}$ is the operator that exchanges \mathbf{S}_1 with \mathbf{S}_2 . In the two-leg ladder it is possible to have in the intermediate state a doubly occupied rung without doubly occupied sites. Thus even for infinite U the exchange coupling is nonzero and

U has to be replaced by the “on-rung” repulsion U_r . In the infinite U case the exchange of spins necessarily involves the exchange of the z -projections of the isospins on two neighboring rungs ($u_1 d_2 \leftrightarrow d_1 u_2$), so the spin-exchange interaction has the form: $\frac{2t^2}{U_r} S_{12} (T_1^+ T_2^- + T_1^- T_2^+)$. Thus, instead of a pure spin-exchange Hamiltonian we obtain a spin-isospin interaction:

$$H_{ST}^{(1)} = A \sum_{\mathbf{n}} (\mathbf{S}_{\mathbf{n}} \cdot \mathbf{S}_{\mathbf{n}+\mathbf{f}_1}) (T_{\mathbf{n}}^x T_{\mathbf{n}+\mathbf{f}_1}^x + T_{\mathbf{n}}^y T_{\mathbf{n}+\mathbf{f}_1}^y). \quad (3)$$

Here, the rungs \mathbf{n} and $\mathbf{n} + \mathbf{f}_1$ are the two nearest-neighbor rungs of the ladder (see Fig. 3) and the interaction amplitude $A = \frac{8t_{\parallel}^2}{U_r}$, U_r being the effective “on-rung” Coulomb repulsion discussed above.

We note that Eq.(3) gives only an approximate description of the spin-isospin interaction in sodium vanadate, because in the presence of inter-rung Coulomb interactions, both initial and intermediate states in the spin-exchange process are complicated many-electron states, so that the increase of the energy in the virtual state cannot be described by a single constant U_r . However Eq.(3) contains many basic ingredients, necessary for a qualitative description of the properties of sodium vanadate.

In particular, treating the spin-isospin interaction in the mean-field approximation we obtain the effective spin-exchange coupling constant:

$$J = A \langle T_{\mathbf{n}}^x T_{\mathbf{n}+\mathbf{f}_1}^x + T_{\mathbf{n}}^y T_{\mathbf{n}+\mathbf{f}_1}^y \rangle, \quad (4)$$

where the brackets denote the thermal and quantum average of the isospin operators. The exchange coupling is, therefore, temperature-dependent, which may account for the deviation of the magnetic susceptibility of sodium vanadate from the Bonner-Fisher curve [10, 26]. Using the Hamiltonian Eq.(1), one can show that, above T_c , the exchange coupling increases as the temperature decreases, which is in agreement with the conclusion of Ref. [26], where such an increase was introduced phenomenologically in order to reconcile the magnetic susceptibility data for NaV_2O_5 with the temperature dependence of the magnetic susceptibility of the Heisenberg spin- $\frac{1}{2}$ chain.

However, there is one very important effect of the electronic charge distribution on the spin exchange that is not described by Eq.(3). Namely, the Hamiltonian Eq.(3) does not explain the spin-gap opening due to the zigzag charge ordering. In order to find the term in the spin-isospin interaction responsible for the spin-gap opening, we note that the exchange between spins on rungs \mathbf{n} and $\mathbf{n} + \mathbf{f}_1$ depends on the position of electrons in the nearest

rungs of the two neighboring ladders, $\mathbf{n} + \mathbf{f}_2$ and $\mathbf{n} + \mathbf{f}_1 - \mathbf{f}_2$ (see Fig. (3)). Roughly speaking, electrons affect the hopping amplitudes between the rungs of nearest-neighbor ladders, which in turn, affect the spin-exchange. The corresponding Hamiltonian describing such an influence has the form:

$$H_{ST}^{(2)} = B \sum_{\mathbf{n}} \left(T_{\mathbf{n}+\mathbf{f}_2}^z - T_{\mathbf{n}+\mathbf{f}_1-\mathbf{f}_2}^z \right) (\mathbf{S}_{\mathbf{n}} \cdot \mathbf{S}_{\mathbf{n}+\mathbf{f}_1}). \quad (5)$$

As was argued in Ref. [7], this interaction is responsible for the opening of the spin gap in the charge ordered phase. Indeed, for the zigzag structure with a doubling of the period in the a and b directions (see Fig. 4a), the exchange alternates along ladders, which opens a spin gap.

To end this section, we note that the virtual hopping of electrons on neighboring rungs, apart from affecting the spin-exchange, also results in corrections to the pure isospin Hamiltonian Eq.(1), which we neglect here, as they are relatively small. Furthermore, for large, but finite on-site Hubbard U , one obtains also the spin-isospin interaction term of the form:

$$H_{ST}^{(3)} = A' \sum_{\mathbf{n}} (\mathbf{S}_{\mathbf{n}} \cdot \mathbf{S}_{\mathbf{n}+\mathbf{f}_1}) T_{\mathbf{n}}^z T_{\mathbf{n}+\mathbf{f}_1}^z, \quad (6)$$

where $A' \propto t_{\parallel}^2/U$.

3 Charge ordering

In this section we ignore spins and discuss the phase diagram for the Hamiltonian (1), which describes the charge dynamics. This is justified as, according to our assumption, the driving force of the transition in sodium vanadate is the electronic charge ordering.

Since the Hamiltonian (1) is real, the average value of $T_{\mathbf{n}}^y$ is zero at all temperatures (unless the time-reversal symmetry is spontaneously broken in the ordered state). On the other hand, $M_{\mathbf{n}}^x = \langle T_{\mathbf{n}}^x \rangle \neq 0$ at all temperatures, due to the presence of the “external” transverse field $2t_{\perp}$. The ordered state of the isospin system is characterized by a nonzero value of $M_{\mathbf{n}}^z = \langle T_{\mathbf{n}}^z \rangle$. The ordering of isospins in the z -direction corresponds to the modulation of the electronic density on the rungs of the vanadium ladders. The type of charge ordering depends on the details of the Coulomb interactions $V_{\mathbf{nm}}$.

If we use as estimates the unscreened Coulomb interactions between electrons, then, according to Eq.(2), the Ising interaction between the isospins

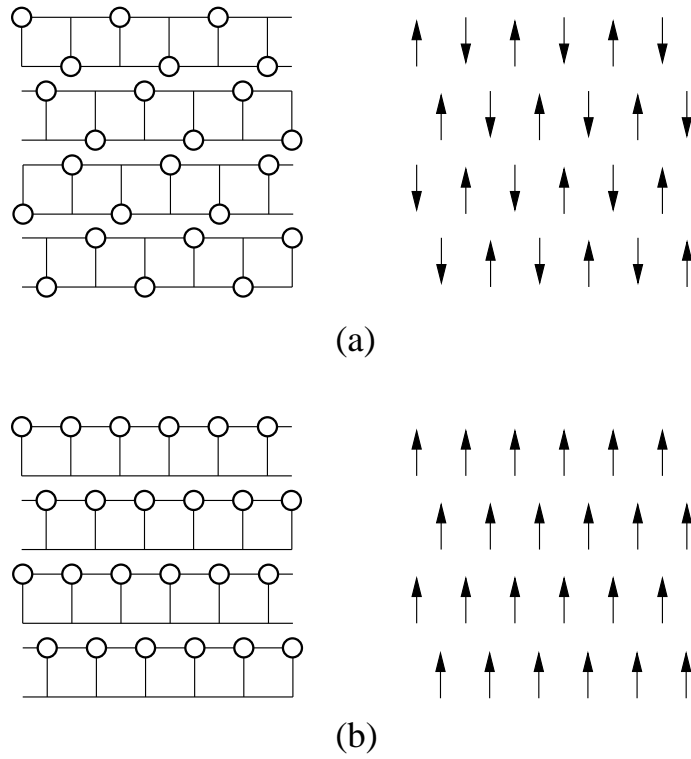


Figure 4: Two charge ordered states: zigzag (or antiferroelectric) ordering with the doubling of the unit cell in the directions a and b (a) and the chain-like (ferroelectric) structure (b). The left part of each picture shows the distribution of the electronic density, while the right part shows the corresponding ordering of isospins.

on the nearest-neighbor rungs in the ladder, $J_A = \frac{1}{4}V_{\mathbf{n},\mathbf{n}+\mathbf{f}_1} = 0.62\text{eV}$. This “antiferromagnetic” interaction favors a zigzag structure, like *e.g.* the one shown in Fig. 4a. On the other hand, the interaction between the isospins on the nearest rungs of two neighboring ladders, $J_F = \frac{1}{4}V_{\mathbf{n},\mathbf{n}+\mathbf{f}_2} = 0.54\text{eV}$, is “ferromagnetic” (for simplicity, we neglect the shifts of vanadium ions out of the basal plane). The “ferromagnetic” interaction favors the structure shown in Fig. 4b, in which electrons occupy with higher probability one chain of each ladder. In general, the charge ordering corresponds to the ordering of the isospins in the z -direction:

$$\langle T_{\mathbf{n}}^z \rangle = e^{i\mathbf{Q}\cdot\mathbf{x}_{\mathbf{n}}} M^z, \quad (7)$$

where $\mathbf{x}_{\mathbf{n}}$ is the position of rung \mathbf{n} , and $\mathbf{Q} = (\frac{\pi}{f_1}, \frac{\pi}{f_2})$ for the zigzag structure, while for the chain structure $\mathbf{Q} = 0$.

If one would take into account only the Ising interactions between the neighboring rungs, then for $J_A > |J_F|$ the energy of the zigzag structure is lower energy than that of the chain structure. However, since the difference between J_A and $|J_F|$ is relatively small, the effects of screening of the Coulomb interactions and the long-range interactions between the isospins are important for the determination of the nature of the charge-ordered state.

Though the precise calculation of the Ising interactions between the isospins is very difficult, one can discriminate between different charge-ordered structures on the basis of the available experimental data. In particular, the chain-like ordering (see Fig. 4b) does not result in the increase of the lattice periodicity in the a and b directions observed in NaV_2O_5 below T_c . Furthermore, the chain structure corresponds to a ferroelectric state. As we shall show below, the optical response of such a system would be quite different from that of sodium vanadate. On the other hand, the zigzag charge ordering results in a doubling of the lattice period in the b -direction. Moreover, if the zigzags in the next-nearest-neighbor ladders have opposite phases (as in Fig. 4a), then the lattice period in the a -direction also doubles.

The generic phase diagram of the Ising model in a transverse field is shown in Fig. 5. For large values of t_{\perp} the system is disordered at all temperatures. For $t_{\perp} < t_{\perp}^*$, the system becomes ordered below some critical temperature T_c . At $t_{\perp} = t_{\perp}^*$ the system has a quantum critical point, at which $T_c = 0$. Since in sodium vanadate the typical values of both the Ising couplings and the hopping amplitude t_{\perp} are of the order of 0.5eV , whereas T_c is only 34K , this material has to be very close to the quantum critical point.

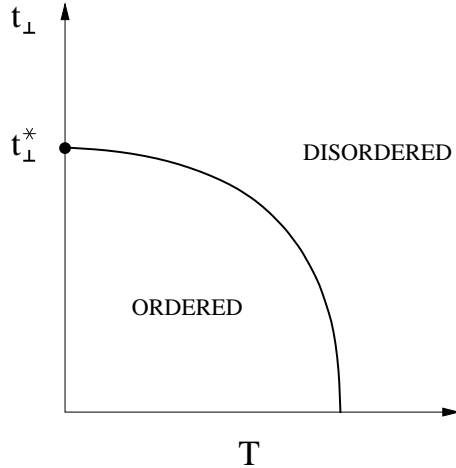


Figure 5: Generic phase diagram of the model described by Eq.(1) in the T - t_{\perp} plane.

The proximity to the quantum critical point may be responsible for the strong dependence of T_c on the hydrostatic pressure observed in sodium vanadate [27, 28]. We note that the fact that the transition temperature is suppressed by pressure can be naturally explained in our model. Both the hopping amplitude t_{\perp} and the amplitudes of the dipolar interactions between the rungs, $V_{\mathbf{nm}}$, increase under pressure. However, t_{\perp} , which involves the overlap of electronic wave functions, depends on the distances between ions more strongly than $V_{\mathbf{nm}}$. Since the hopping amplitude tends to disorder the system, the transition temperature decreases under pressure.

The isospin Hamiltonian Eq.(1) is the Hamiltonian of the Ising model with long-range interactions in a transverse field. Recently, a considerable progress was made in the calculation of the linear response functions of such systems, which close to a quantum critical point, become to a large extent [29]. While those results could be useful to describe the response function at wave vectors \mathbf{q} close to \mathbf{Q} (*e.g.*, the temperature dependence of the shape of neutron diffraction peaks), in this paper we are mostly interested in the dielectric and magnetic susceptibility of sodium vanadate at $\mathbf{q} = 0$, as the latter is measured in optical experiments. We use the random phase approximation (RPA) to obtain the necessary correlation functions of the isospin operators. Then, for our purposes, it is sufficient to describe the ordered state in the mean field approximation.

In this approximation $M_{\mathbf{n}}^x$ and $M_{\mathbf{n}}^z$ are found from

$$\begin{cases} 2t_{\perp}M_{\mathbf{n}}^z + M_{\mathbf{n}}^x \sum_{\mathbf{m}} V_{\mathbf{nm}} M_{\mathbf{m}}^z = 0, \\ M_{\mathbf{n}} = \sqrt{(M_{\mathbf{n}}^x)^2 + (M_{\mathbf{n}}^z)^2} = \frac{1}{2} \tanh \frac{H_{\mathbf{n}}}{2T}. \end{cases} \quad (8)$$

The first equation fixes the orientation of the vector $\langle \mathbf{T}_{\mathbf{n}} \rangle$, which has to be parallel to the vector of the “field” applied to the isospin at the site \mathbf{n} , $\mathbf{H}_{\mathbf{n}} = (2t_{\perp}, 0, -\sum_{\mathbf{m}} V_{\mathbf{nm}} M_{\mathbf{m}}^z)$. The second equation gives the length of $\langle \mathbf{T}_{\mathbf{n}} \rangle$ (in that equation $H_{\mathbf{n}} = |\mathbf{H}_{\mathbf{n}}|$).

Above T_c we have

$$\begin{cases} M_{\mathbf{n}}^x = \frac{1}{2} \tanh \frac{t_{\perp}}{T}, \\ M_{\mathbf{n}}^z = 0, \end{cases} \quad (9)$$

while for the ordered states shown in Fig. 4, the order parameter is given by Eq.(7) and $M_{\mathbf{n}}^x$ is constant below T_c :

$$M_{\mathbf{n}}^x = M^x = \frac{2t_{\perp}}{|V(\mathbf{Q})|}. \quad (10)$$

The absolute value of the magnetization, $M = \sqrt{(M^x)^2 + (M^z)^2}$, satisfies

$$M = \frac{1}{2} \tanh \frac{\sqrt{(2t_{\perp})^2 + (M^z V(\mathbf{Q}))^2}}{2T}, \quad (11)$$

where $V(\mathbf{Q})$ is the value of the Fourier transform of $V_{\mathbf{nm}}$ at $\mathbf{q} = \mathbf{Q}$:

$$V(\mathbf{Q}) = \sum_{\mathbf{n}} e^{-i\mathbf{Q}\cdot(\mathbf{x}_{\mathbf{n}}-\mathbf{x}_{\mathbf{m}})} V_{\mathbf{nm}}. \quad (12)$$

Finally, at the critical temperature

$$2t_{\perp} + M^x(T_c)V(\mathbf{Q}) = 0, \quad (13)$$

where $M^x(T)$ is given by Eq.(9). Clearly, $V(\mathbf{Q})$ has to be negative and $V(\mathbf{q})$ has to have a minimum at $\mathbf{q} = \mathbf{Q}$ (the location of the minimum determines the type of the charge-ordered structure). Furthermore, Eq.(13) only has a solution for $|V(\mathbf{Q})| \geq 4t_{\perp}$. In other words, in the mean field approximation, the critical point is reached at $t_{\perp}^* = \frac{|V(\mathbf{Q})|}{4}$.

4 Isospin excitations

The isospin excitations described by the Hamiltonian (1) are the rung excitons, *i.e.* the electronic excitations from the symmetric state with energy $-t_\perp$ to the antisymmetric state with energy $+t_\perp$, which can propagate from rung to rung due to the Coulomb interactions between the electrons. This can be most easily understood by performing a rotation in the isospin space around the y -axis, under which $T^x \rightarrow T^z$ and $T^z \rightarrow -T^x$ (see Appendix A). Then the excitation from the symmetric to the antisymmetric electron state on a rung corresponds to a spin flip. Due to the Ising interaction between the isospins on different rungs, which in the new basis has the form, $\frac{1}{2} \sum_{\mathbf{nm}} V_{\mathbf{nm}} T_n^x T_m^x$, the spin flip can hop from rung to rung.

The dispersion of these excitations can be found, *e.g.*, by considering the retarded Green function

$$\langle\langle T^z | T^z \rangle\rangle_{\omega, \mathbf{q}} = -i \int_0^\infty dt e^{i(\omega+i\delta)t} \sum_{\mathbf{n}} e^{-i\mathbf{q}\cdot\mathbf{x}_n} \langle [T^z(t), T^z(0)] \rangle \quad (14)$$

(here we use the original basis in the isospace). This Green function is calculated in the random phase approximation (RPA) in Appendix A (see Eqs. (33) and (42)). From the poles of the RPA Green function we obtain the energy of the isospin excitation with wave vector \mathbf{q} , valid both above and below T_c :

$$E_{\mathbf{q}} = \sqrt{(2t_\perp)^2 + 2t_\perp M^x V(\mathbf{q}) + (|V(\mathbf{Q})| M^z)^2}, \quad (15)$$

where the averages M^x and M^z are given by Eq.(9) above T_c and Eqs.(10) and (11) below T_c .

Since the energy of the electron excitation on a rung, $2t_\perp \sim 0.7\text{eV}$ [16], is rather large, the isospin excitations are irrelevant for the low-temperature properties of sodium vanadate, unless this large energy is compensated by a large band width (the latter is determined by the amplitude of the variation of $V(\mathbf{q})$, which for sodium vanadate is also expected to be of the order of 1eV). We thus assume, that close to the bottom of the exciton band (*i.e.*, for $\mathbf{q} \sim \mathbf{Q}$), the exciton energy is comparable to temperature (or smaller).

The existence of soft isospin excitations implies a strong temperature dependence of the exciton gap, $\Delta = E_{\mathbf{Q}}$. The typical temperature dependence of the isospin gap is shown in Fig. 6. Above T_c the ‘‘transverse magnetization’’ M^x grows when temperature decreases (see Eq.(9)), which results in a decrease of the gap (we recall that $V(\mathbf{Q})$ in Eq.(15) is negative). At the

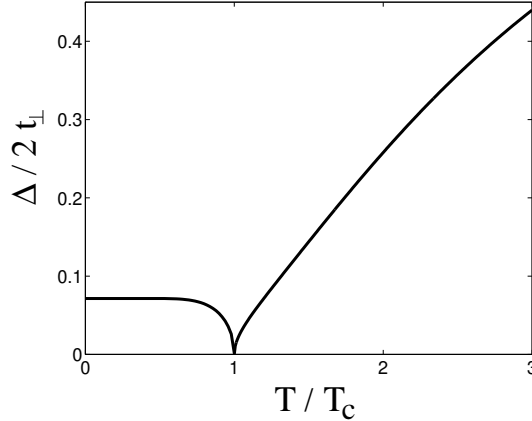


Figure 6: Temperature dependence of the isospin gap Δ . The value of $|V(\mathbf{Q})|$, used for this calculation, is close to its quantum critical value, $2t_{\perp}$, so that the isospin gap $\Delta \ll 2t_{\perp}$.

transition temperature, T_c , the exciton gap disappears in accordance with Eq.(13). Below T_c , the order parameter, M^z , increases as temperature decreases, while M^x stays constant (see Eqs. (10) and (11)). As a result the exciton gap again reappears.

5 Anomaly of dielectric susceptibility at T_c

The isospin excitations discussed in the previous section can be excited by applying an electric field in the direction of the rungs (a -direction). Within the isospin model the interaction with such a field, $E_a(t)$, is described by the Hamiltonian

$$H_{int} = elE_a(t) \sum_{\mathbf{n}} T_{\mathbf{n}}^z, \quad (16)$$

where $l \approx \frac{a}{3}$ is the length of the rung. Then the contribution to the dielectric susceptibility of the electrons occupying the d_{xy} orbitals on the vanadium sites is:

$$\chi_a(\omega, \mathbf{q}) = -C \langle \langle T^z | T^z \rangle \rangle_{\omega, \mathbf{q}}, \quad (17)$$

where the constant $C = \frac{2e^2 l^2}{abc}$, a , b , and c being the lattice constants of the high-temperature unit cell, and the retarded Green function $\langle \langle T^z | T^z \rangle \rangle_{\omega, \mathbf{q}}$ above and below T_c is given by Eqs. (33) and (42), respectively. Using these

equations we obtain

$$\chi_a(\omega, \mathbf{q}) = -C \frac{2t_{\perp} M^x}{(\omega^2 - E_{\mathbf{q}}^2 + i\delta \text{sign}\omega)} \quad (18)$$

for the charge susceptibility above T_c (here, M^x is given by Eq.(9)) and

$$\chi_a(\omega, \mathbf{q}) = -C \frac{(2t_{\perp})^2}{|V(\mathbf{Q})|} \frac{1}{(\omega^2 - E_{\mathbf{q}}^2 + i\delta \text{sign}\omega)} \quad (19)$$

below T_c .

The frequency dependence of the dielectric susceptibility was measured by optical absorption [21, 22, 30]. Its imaginary part shows a rather broad peak at energy $\sim 1\text{eV}$, which was assigned in Ref. [21] to bonding-antibonding excitations of electrons on rungs. According to Eq.(18) the peak should be located at the energy of the isospin excitations with $\mathbf{q} = 0$. As for the zigzag structure, shown in Fig. 4a, this excitation lies far from the bottom of the exciton band, located at $\mathbf{Q} = (\frac{\pi}{f_1}, \frac{\pi}{f_2})$, its energy, $E_{\mathbf{q}=0}$, should indeed be rather large ($\sim 2t_{\perp}$). On the other hand, for the chain structure (see Fig. 4b) the bottom of the exciton band would be at $\mathbf{q} = 0$ and the soft isospin excitations would result in a strong peak in the optical absorption at low energy, $E_{\mathbf{q}=0} \approx 0$, which is not observed in these experiments.

The type of charge ordering also determines the type of the anomaly in the temperature dependence of the static dielectric susceptibility close to T_c . Such an anomaly appears due to the redistribution of charge at the phase transition. The order parameter M^z , as well as M^x and the isospin energy $E_{\mathbf{q}}$ depend on T , which makes the dielectric susceptibility temperature-dependent (see Eqs.(18) and (19)).

For the antiferroelectric ordering of charges, as in the case of the zigzag ordering (see Fig. 4a), the susceptibility to the uniform field is finite at T_c (see Eq.(18) with $E_{\mathbf{q}=0}$ finite), while its temperature derivative has a discontinuity at the transition temperature, as is shown in Fig. 7. (This is analogous to the anomaly in the magnetic susceptibility of the Ising antiferromagnet). On the other hand, for the ferroelectric type of ordering, such as the chain-like structure shown on Fig. 4b, the susceptibility would diverge at T_c . The anomaly in the temperature dependence of the dielectric susceptibility of NaV_2O_5 has been measured at microwave and far-infrared frequencies [11, 12, 13]. The observed anomaly is similar to that shown in Fig. 7 and

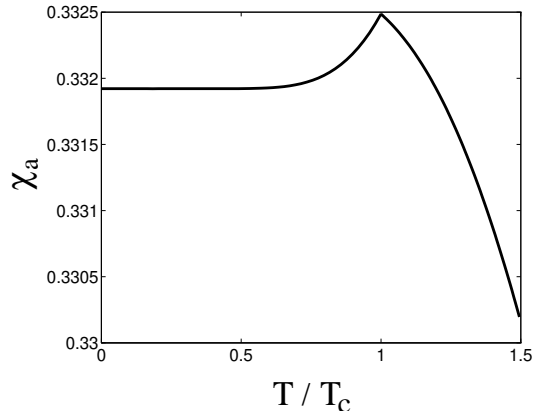


Figure 7: The typical temperature dependence of the static dielectric susceptibility to electric fields applied in the a -direction calculated in the RPA approximation. The parameters of the isospin Hamiltonian were chosen such that the value of T_c is much smaller than t_{\perp} .

consistent with a charge ordering of the antiferroelectric type [11], although above T_c the dielectric susceptibility of sodium vanadate continues to grow with temperature, whereas the RPA predicts a decrease.

6 Optical absorption at low energies

A remarkable feature of the optical absorption spectrum of sodium vanadate at low-energies is that the low-energy shoulder of the peak at 8000cm^{-1} extends all the way down to $\sim 3000\text{cm}^{-1}$ (see Fig. 8). Furthermore, at lower frequencies there is another broad absorption band stretching from $\sim 100\text{cm}^{-1}$ up to $\sim 1500\text{--}2000\text{cm}^{-1}$ with a maximum at $\sim 300\text{cm}^{-1}$ [21, 22]. A very broad peak with a maximum at 600cm^{-1} is also observed in Raman scattering [23, 22, 24]. The large width of these peaks, as well as a number of the Fano resonances observed in the far-infrared absorption spectrum [22, 21], indicate the presence of a broad continuum of low-energy excitations in sodium vanadate, which covers, practically, the whole midinfrared range of frequencies.

The low-energy continuum, observed both above and below T_c , can, in principle, be due to the photoexcitation of several isospin excitations lying close to the bottom of the exciton band. To describe such processes one has to go beyond the RPA. Then the one-exciton states are mixed with the states

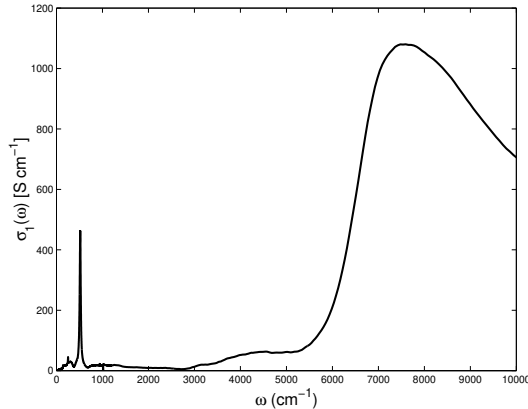


Figure 8: The frequency dependence of the real part of the optical conductivity of NaV₂O₅ at 300K in the midinfrared range (courtesy of Prof. D. van der Marel [21]).

containing three, five, and more excitons. However, since the number of excitons created in the photoabsorption is odd, the momentum conservation does not allow all of them simultaneously to have low energy. Thus, the pure exciton continuum should begin at rather high energies and cannot account for the mid-infrared continuum in sodium vanadate.

To substantiate the point that the isospin excitations alone cannot give rise to the observed low-energy optical absorption, we consider an isolated vanadium ladder with the isospin Hamiltonian:

$$H_T = -2t_{\perp} \sum_n T_n^x + V \sum_n T_n^z T_{n+1}^z.$$

For open boundary conditions, this Hamiltonian can be diagonalized exactly. To this end we first perform a rotation around the y -axis in the isospin space (*cf.* Appendix). The resulting Hamiltonian is diagonalized by transforming the isospins to fermions (using the Jordan-Wigner transformation) and then applying the Bogoliubov transformation [33]. The exact dispersion of the fermionic excitations reads:

$$E_q = \sqrt{\left(2t_{\perp} + \frac{V}{2} \cos q\right)^2 + \left(\frac{V}{2} \sin q\right)^2},$$

with q a quantum number that follows from a transcendental equation [33], and which lies in the interval $0 < q < \pi$. Thus, the isospin gap is given by

$$\Delta = E_{\pi} = \left|2t_{\perp} - \frac{V}{2}\right|.$$

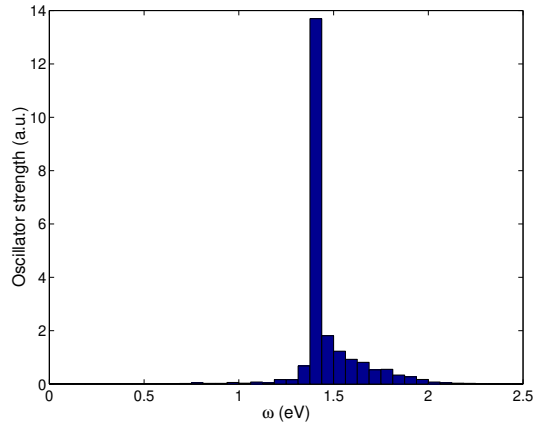


Figure 9: The oscillator strength for an isolated two-leg ladder of $N = 70$ rungs with very small value of the isospin gap at $q = \pi$ (see explanations in the text). The narrow peak is due to the single exciton absorption. The absorption above the main peak is due to the photoexcitation of three excitons. The very small oscillator strength for the frequencies below the frequency of the main peak is due to the one-exciton absorption and is a finite-size effect.

The oscillator strength of a n -exciton state (n odd) may now be expressed in terms of the ground state expectation value of strings of Fermi operators. The latter may be evaluated using Wick's theorem which results in determinants of matrices with components that follow from the Bogoliubov transformation coefficients. For the 1- and 3-exciton states, this calculation has been performed explicitly in Ref. [34]. Using these results, we find for a ladder of $N = 70$ rungs and $2t_{\perp} = 0.7\text{eV}$ the absorption spectrum plotted in Fig. 9. As NaV_2O_5 seems to be close to the quantum critical point, $2t_{\perp} = \frac{V}{2}$, (see discussion in Sec. 3), we choose $\frac{V}{2} = 0.6999\text{eV}$, which gives an isospin gap 10^{-4}eV . The narrow peak is due to the single-exciton absorption. The absorption above the main peak is due to the photoexcitation of three excitons. This process contributes to the broad high-energy wing of the main absorption peak observed in sodium vanadate [21]. The small oscillator strength at frequencies below the frequency of the main peak is due to the one-exciton absorption and is a finite-size effect (breaking of the momentum selection rule). For small photon frequencies the absorption due to the 5-exciton states is negligible due to the small phase volume of these states.

In Ref. [21] the low-energy optical was associated with the two-spinon

continuum. Since magnetic excitations cannot be directly induced by photon absorption, the authors of Ref. [21] invoked the so-called “charged magnon” mechanism. The corresponding Feynman diagram is shown in Fig.10(a): The process involves the creation of a virtual high-energy isospin excitation with $\mathbf{q} = 0$, which then decays into two spinons. However, the coupling of the isospin excitation with zero wave vector to spinons is only nonzero if the system has a permanent electric dipole. In other words, the magnons have charge only if sodium vanadate is ferroelectric, which would require the chain-like electronic ordering (cf. Fig 4b) both above and below T_c . For a long time sodium vanadate was, indeed, believed to have such a chain structure [1]. However, this structure was found to be inconsistent (certainly, in the high-temperature phase) with recent experimental data (see discussion in Sec. 5).

Thus the coupling of a photon with zero wave vector to two spinons is zero, and we have to find another mechanism for the low-energy optical absorption. In the remainder of this section, we shall show that the low-energy absorption may result from the photoexcitation of a three-particle continuum: two spinons and one low-energy isospin excitation. This mechanism is illustrated by the diagram in Fig.10(b). This process also takes place via a virtual isospin excitation with zero wave vector and high energy E_0 , which then decays into a low-energy isospin excitation with the wave vector \mathbf{q} close to the bottom of the band, $\mathbf{q} \sim \mathbf{Q}$, and two spin excitations, which carry the momentum $-\mathbf{q}$. Alternatively, the thermally excited isospin excitation can be annihilated in the process of optical absorption (see Fig.10(c)).

Our mechanism requires the coupling of *two* isospin excitations (one of high energy, another of low energy) to two spin excitations. In sodium vanadate such a coupling results from the fact that the spin exchange of electrons on neighboring rungs of a two-leg ladder cannot be separated from the exchange of their isospins. The Hamiltonian describing the spin-isospin coupling was discussed in Sec. 2. As an exact treatment of the spin-isospin model is not possible we use a number of approximations to calculate the optical absorption spectrum. First we note that the Hamiltonian of the spin-isospin interaction given by Eqs. (3), (5), and (6) can be written in the form:

$$H_{ST} = H_{ST}^{(1)} + H_{ST}^{(2)} + H_{ST}^{(3)} = \sum_{\mathbf{n}} \mathcal{T}_{\mathbf{n}} \mathcal{S}_{\mathbf{n}},$$

where $\mathcal{T}_{\mathbf{n}}$ contains all isospin operators:

$$\mathcal{T}_{\mathbf{n}} = A \left(T_{\mathbf{n}}^x T_{\mathbf{n}+\mathbf{f}_1}^x + T_{\mathbf{n}}^y T_{\mathbf{n}+\mathbf{f}_1}^y \right) + A' T_{\mathbf{n}}^z T_{\mathbf{n}+\mathbf{f}_1}^z + B \left(T_{\mathbf{n}+\mathbf{f}_2}^z - T_{\mathbf{n}+\mathbf{f}_1-\mathbf{f}_2}^z \right), \quad (20)$$

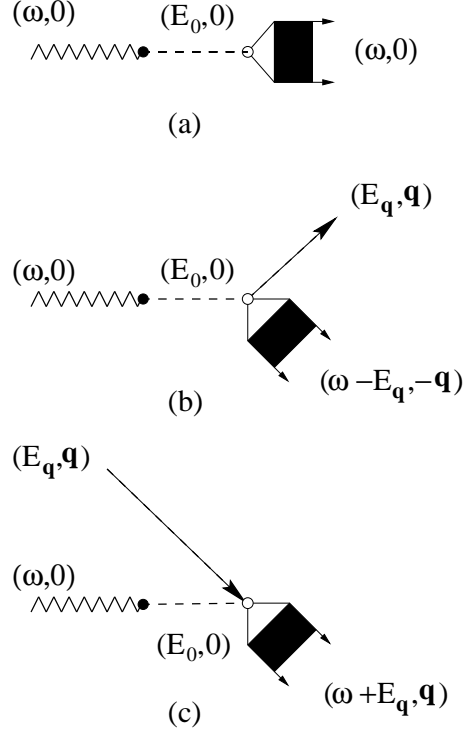


Figure 10: Diagrams describing: (a) the “charged magnon” mechanism, (b) the photoexcitation of the two-spinon continuum and a low-energy exciton, and (c) the photoexcitation of the two-spinon continuum with the annihilation of a low-energy exciton. The wavy and dashed lines correspond to, respectively, a photon and a charge exciton, while the black square indicates the two-spinon continuum.

and

$$\mathcal{S}_{\mathbf{n}} = \mathbf{S}_{\mathbf{n}} \cdot \mathbf{S}_{\mathbf{n}+\mathbf{f}_1}.$$

Although in our model the spin dynamics is inseparable from the dynamics of the isospins, we may, however, obtain a “pure spin Hamiltonian” by treating the isospin operators in H_{ST} within the mean-field approximation:

$$H_S = \sum_{\mathbf{n}} J_{\mathbf{n},\mathbf{n}+\mathbf{f}_1} (\mathbf{S}_{\mathbf{n}} \cdot \mathbf{S}_{\mathbf{n}+\mathbf{f}_1}), \quad (21)$$

where the effective spin-exchange constant is obtained by the thermal average of $\mathcal{T}_{\mathbf{n}}$ over the state of the isospin system:

$$J_{\mathbf{n},\mathbf{n}+\mathbf{f}_1} = \langle \mathcal{T}_{\mathbf{n}} \rangle_{H_T}.$$

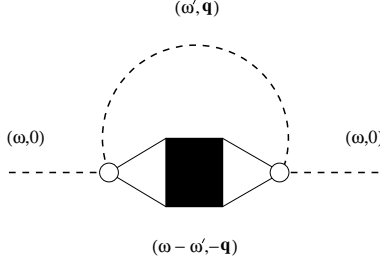


Figure 11: The diagram describing the correction to the Green function of the isospin excitation due to scattering on the spin excitations. This correction which gives rise to low-energy optical absorption.

As was already discussed in Sec. 2, the thus obtained spin-exchange constant depends on temperature and becomes alternating along the spin chains below T_c . Since according to our assumption the charge ordering is mainly driven by the pure isospin Hamiltonian H_T , we neglect the effect of the spin-isospin interactions on the state of the isospin system. The remaining part of the spin-isospin Hamiltonian (the residual interaction) describes the scattering of isospin excitations on spin excitations. This scattering gives rise to the low-energy absorption and will be treated as a perturbation.

In this paper we consider the optical absorption only above T_c (*i.e.*, no charge ordering and no spin gap). Furthermore, the isospin excitations are treated as bosons. In particular, the operator

$$T_{\mathbf{q}}^z = \frac{1}{\sqrt{N}} \sum_{\mathbf{n}} e^{-i\mathbf{q}\mathbf{x}_{\mathbf{n}}} T_{\mathbf{n}}^z$$

annihilates the isospin excitation with the wave vector \mathbf{q} and creates such an excitation with the wave vector $-\mathbf{q}$:

$$T_{\mathbf{q}}^z \sim \sqrt{\frac{t_{\perp} M}{E_{\mathbf{q}}}} (b_{-\mathbf{q}}^{\dagger} + b_{\mathbf{q}}).$$

The coefficient in the right-hand side of the last equation was found by comparison of this equation with the Green function Eq.(33).

Since the operator $T_{\mathbf{n}}$ (see Eq.(20)) contains products of two isospin operators, it either results in the creation and annihilation of two isospin excitations, or in the scattering of the isospin excitation. In particular, if one of the isospin excitations has zero wave vector (as is the case in the optical

absorption), then

$$\mathcal{T}_{\mathbf{q}} \sim g_{\mathbf{q}} \frac{t_{\perp} M}{\sqrt{E_0 E_{\mathbf{q}}}} (b_{-\mathbf{q}}^{\dagger} + b_{\mathbf{q}}) (b_0^{\dagger} + b_0),$$

where $g_{\mathbf{q}}$ is the coupling constant.

To lowest order in the residual spin-isospin interaction, the Green function of the isospin excitation obtains the correction shown in Fig. 11, which leads to the low-energy optical absorption described by the diagrams in Figs. 10 (b) and (c). The corresponding contribution to the imaginary part of the dielectric susceptibility is:

$$\begin{aligned} \Delta\chi_a''(\omega, 0) &= \frac{K}{N} \sum_{\mathbf{q}} \frac{|g_{\mathbf{q}}|^2}{E_0 E_{\mathbf{q}}} \left[\chi_S''(\omega - E_{\mathbf{q}}, -\mathbf{q}) \left(\coth \frac{E_{\mathbf{q}}}{2T} - \coth \frac{(E_{\mathbf{q}} - \omega)}{2T} \right) \right. \\ &\quad \left. + \chi_S''(\omega + E_{\mathbf{q}}, \mathbf{q}) \left(\coth \frac{E_{\mathbf{q}}}{2T} - \coth \frac{(E_{\mathbf{q}} + \omega)}{2T} \right) \right]. \end{aligned} \quad (22)$$

Here, the first term in square brackets is due to photoexcitation of one low-energy exciton plus two spinons (see Fig. 10b), while the second term describes annihilation of a thermally excited low-energy excitation, accompanied by the creation of two spin excitations (see Fig. 10c). In Eq.(22) we have defined

$$K = \frac{1}{abc} \left(\frac{2elt_{\perp}^2 M^2}{E_0^2 - \omega^2} \right)^2,$$

while $\chi_S(\omega, \mathbf{q}) = \chi_S(\omega, q_1)$ is the susceptibility of the Heisenberg spin- $\frac{1}{2}$ chain:

$$\chi_S(\omega, q_1) = i \int_0^{\infty} dt e^{i\omega t - iq_1 n} \langle [\mathcal{S}_n(t), \mathcal{S}_0(0)] \rangle_{H_S} \quad (23)$$

(here q_1 is the wave vector in the chain direction measured in units of $\frac{1}{b}$). Since no exact expression for this susceptibility is known that holds for all values of q , ω , and T , we calculate it by substituting the Heisenberg model by the renormalized XY model, which is equivalent to a half-filled chain of spinless fermions with the dispersion $\varepsilon(k) = -pJ \cos k$, where $p = 1 + 2/\pi$ [31]. Then

$$\mathcal{S}_n \rightarrow -\frac{p}{2} (c_{n+1}^{\dagger} c_n + c_n^{\dagger} c_{n+1}),$$

and

$$\chi_S''(\omega, q) = \frac{p^2}{4} \int_{-\pi}^{\pi} dk \delta(\omega + \varepsilon_k - \varepsilon_{k+q}) \cos^2 \left(k + \frac{q}{2} \right) \left[\tanh \frac{\varepsilon_{k+q}}{2T} - \tanh \frac{\varepsilon_k}{2T} \right].$$

According to our assumption, the isospin excitations only are soft in a small vicinity of $q_1 = \pi$. Then the wave vector of the spin excitations in the low-energy continuum is also close to π , in which case the analytical expression for the imaginary part of the spin susceptibility is:

$$\chi''_S(\omega, \pi) = \theta(\Omega^2 - \omega^2) \frac{p^2}{\Omega} \sqrt{1 - \left(\frac{\omega}{\Omega}\right)^2} \tanh \frac{\omega}{4T}. \quad (24)$$

Here, $\Omega = 2pJ$ is the bandwidth of the spinless fermions, which corresponds to the maximal energy of the two-spinon excitation in the Heisenberg model.

In Fig. 12, we show the real part of optical conductivity, $\sigma_1(\omega) \propto \omega \chi''_a(\omega, 0)$, resulting from Eqs. (22) and (24) for the model parameters: $\Delta = 200\text{K}$, $T = 300\text{K}$, and $J = 560\text{K}$ is shown Fig. 12. The spectrum has two singularities at $\omega = \Omega \pm \Delta$ due to the fact that the maximal energy carried by two spin excitations cannot exceed Ω . The contribution of the process with the annihilation of an isospin excitation (see Fig. 10c) has its maximum at $\omega \sim \Omega$ and decreases exponentially (as $e^{-\beta\omega}$) at larger frequencies. Therefore, the absorption at $\Omega, T \ll \omega \ll E_0$ is entirely due to the process shown in Fig. 10b. At these frequencies the optical absorption spectrum measures, basically, the density of isospin excitations. Since the spectrum of these excitations stretches from very low energies near the bottom of the band at $\mathbf{q} = \mathbf{Q}$ up to the energies of the order of $2t_\perp$, a (relatively small) optical absorption due to the photoexcitation of the three-particle continuum should occur at all frequencies between Δ and E_0 . This explains the midinfrared absorption continuum observed in NaV_2O_5 and described in the beginning of this section. We note that, in agreement with our theory, this continuum is only observed when the electric field is directed along the ladder rungs (along **a**).

To end this section, we point out, that our mechanism of the optical absorption at low photon energies is very similar to the Lorenzana-Sawatzky mechanism of the phonon-mediated photoexcitation of two magnons [35]. The difference lies in the fact that the phonon dispersion is usually small or comparable to that of magnons, so that the shape of the three-particle continuum is mainly determined by the spin excitations [36]. On the other hand, in our case the shape of the optical spectrum is governed by the isospin excitations, which have a much wider band than spinons.

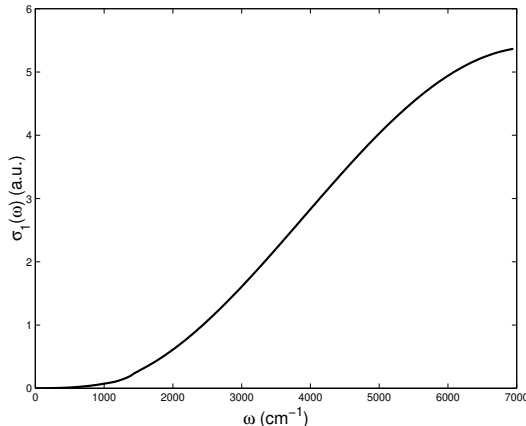


Figure 12: The low-energy part of the optical absorption spectrum due to the process shown in Figs.10(b) and (c).

7 Discussion and Conclusions

In this paper we discussed the spin-isospin model of sodium vanadate. We showed that when the rungs of the vanadium two-leg ladders are occupied mostly by a single electron, the spectrum of low-energy excitations may include, not only spin, but also charge excitations. The latter are the bonding-antibonding electronic excitations on the ladder rungs, which become itinerant due to the Coulomb interactions between electrons on different rungs.

We described the dynamics of these excitations with isospin- $\frac{1}{2}$ operators. The isospin Hamiltonian is identical to the Hamiltonian of the Ising model in a transverse field. In this model one obtains a transition into an ordered state at low temperatures, which corresponds to the charge ordering of electrons on rungs of the vanadium ladders. At the transition temperature the spectrum of the isospin excitations becomes gapless.

Furthermore, we showed that the dynamics of the spins and isospins are coupled to each other. A pure spin exchange does not exist - the exchange of spins necessarily involves the exchange of isospins. As a result the effective spin exchange constants depend on temperature. Below the charge ordering temperature the spin exchange constants alternate along ladders, which opens a spin gap.

As we have shown, the spin-isospin Hamiltonian explains the anomaly in the dielectric susceptibility at T_c and the optical absorption at low frequencies, observed in sodium vanadate. The shape of the anomaly in the

dielectric constant proves that the charge ordering below T_c in NaV_2O_5 is of an antiferroelectric (zigzag) type.

A considerable part of this paper was devoted to the calculation of the optical absorption within the spin-isospin model. We argued that neither pure isospin excitations, nor pure spin excitations can explain the broad bands in the optical absorption spectrum of sodium vanadate found in the whole range of mid-infrared frequencies. We showed that this absorption can be due to the photoexcitation of a three-particle continuum (one low-energy exciton and two spinons). We also note that below T_c , the quasi-momentum conservation allows for the optical excitation of a single low-energy excitation, as the increase of the lattice period folds these modes into the zone center. Indeed, both in optical absorption [32] and Raman spectra [24], several lines have been observed whose intensity shows an anomalous temperature dependence.

Thus the spin-isospin model allows us to explain qualitatively the main experimental facts on sodium vanadate, *i.e.*, the charge ordering, the spin-gap opening, and the low-energy absorption. The main difficulty of this model is to explain the low value of the charge ordering temperature. One possibility mentioned above is the proximity to the quantum critical point, which, however, requires a fine tuning of the model parameters (the transverse field and the Ising interaction between the isospins). Another possibility, the frustration of the Ising interactions due to the relative shifts between neighboring ladders, will be discussed in detail elsewhere.

In conclusion, in sodium vanadate the electronic charge dynamics seems to play an important role, and the coupling between the charge and spin degrees of freedom is crucial in understanding the properties of this material. Finally, we note that a similar spin-isospin model could be used to describe the interplay between the charge and antiferromagnetic ordering in the quasi-two-dimensional organic system $\kappa\text{-(BEDT-TTF)}_2\text{X}$ (see, *e.g.*, [37, 38]), in which the role of the V rungs is played by dimers of BEDT-TTF molecules.

This work is supported by the “Stichting voor Fundamenteel Onderzoek der Materie (FOM)” and the MCS+ programme. The authors are grateful to B. Büchner, C. Gros, W. Kremer, P. van Loosdrecht, D. van der Marel, T. Palstra, and N. Prokof’ev for fruitful discussions.

References

- [1] A. Carpy and J. Galy, Acta Crystallogr. B **31**, 1481 (1975).
- [2] M. Isobe and Y. Ueda, J. Phys. Soc. Jpn. **65**, 1178 (1996).
- [3] Y. Fujii et al., J. Phys. Soc. Jpn. **66**, 326 (1997).
- [4] B.K. Chakravery, M.J. Sienko, and J. Bonnerot, Phys. Rev. B **17**, 3781 (1978).
- [5] T. Ohama, H. Yasuoka, M. Isobe, and Y. Ueda, Phys. Rev. B **59**, 3299 (1999); preprint cond-mat/0003141.
- [6] H. Seo and H. Fukuyama, J. Ph. Soc. Jpn. **67**, 2602 (1998).
- [7] M. Mostovoy and D. Khomskii, Solid State Commun. **113**, 159 (2000).
- [8] J. Hemberger *et al.*, Europhys. Lett. **42**, 661 (1998).
- [9] W. Schnelle, Yu. Grin, and R. Kremer, Phys. Rev. B **59**, 73 (1999).
- [10] B. Büchner *et al.*, unpublished.
- [11] A.I. Smirnov *et al.*, Phys. Rev. B., **59**, 14546 (1999).
- [12] Y. Sekine *et al.* Technical report ISSP ser. A N3371 (1998), submitted to Journ. Phys. Soc. Jpn.
- [13] M. Poirier, P. Fertey, J. Jegoudez, and A. Revcolevschi, Phys. Rev. B **60**, 7341 (1999).
- [14] A. Meetsma, J.L. de Boer, A. Damascelli, T. T. M. Palstra, J. Jegoudez, and A. Revcolevschi, Acta Cryst. C **54**, 1558 (1998).
- [15] H.G. Schnering *et al.*, Z. Kristallogr. **213**, 246 (1998).
- [16] H. Smolinski *et al.*, Phys. Rev. Lett. **80**, 5164 (1998).
- [17] J. Lüdecke *et al.*, Phys. Rev. Lett. **82**, 3633 (1999).
- [18] J.L. de Boer *et al.*, Phys. Rev. Lett. **84**, 3962 (2000).
- [19] J.L. de Boer *et al.*, preprint cond-mat/0008054.

- [20] R. Blinc and B. Žekš, “Soft Modes in Ferroelectrics and Antiferroelectrics”, North-Holland, Amsterdam (1974).
- [21] A. Damascelli *et al.*, Phys. Rev. Lett. **81**, 918 (1998).
- [22] M.N. Popova *et al.*, JETP **88**, 1186 (1999) [Zh. Eksp. Teor. Fiz. **115**, 2170 (1999)].
- [23] S. Golubchik *et al.*, J. Phys. Soc. Jpn. **66**, 4042 (1997).
- [24] M. Fisher *et al.*, Phys. Rev. B **60**, 7284 (1999).
- [25] K.I. Kugel and D.I. Khomskii, Sov. Phys. JETP **37**, 725 (1973); Sov. Phys.-Uspekhi **25**, 231 (1982).
- [26] D. C. Johnston *et al.*, Phys. Rev. B **61**, 9558 (2000).
- [27] H. Nakao *et al.*, Physica B **241-243**, 534 (1998).
- [28] I. Loa *et al.*, Phys. Rev. B **60**, R6945 (1999).
- [29] S. Sachdev, Phys. Rev. B **55**, 142 (1997); Phys. Rev. Lett. **78**, 2220 (1997).
- [30] M. N. Popova *et al.*, JETP Lett. **65**, 743 (1997) [Pis'ma Zh. Eksp. Teor. Fiz. **65**, 711 (1997)].
- [31] L. N. Bulaevskii, Zh. Eksp. Theor. Fiz. **43**, 968 (1962) [Sov. Phys. JETP **16**, 685 (1963)].
- [32] M. N. Popova, A. B. Sushkov, and S. A. Golubchik, (private communication).
- [33] E. Lieb, T. Schultz, and D. C. Mattis, Ann. Phys. **16**, 407 (1961).
- [34] L. D. Bakalis and J. Knoester, J. Chem. Phys. **106**, 6964 (1997).
- [35] J. Lorenzana and G. A. Sawatzky, Phys. Rev. Lett. **74**, 1867 (1995).
- [36] H. Suzuura *et al.*, Phys. Rev. Lett. **76**, 2579 (1996).
- [37] H. Kino and H. Fukuyama, J. Phys. Soc. Jpn. **65**, 2158 (1996).
- [38] R. H. McKenzie, Comments Cond. Mat. Phys. **18**, 309 (1998).

[39] D. N. Zubarev, Sov. Phys. Uspekhi **3**, 320 (1960) [Usp. Fiz. Nauk **71**, 71 (1960)].

[40] S. B. Haley and P. Erdös, Phys. Rev. B **5**, 1106 (1972).

A Spectrum of isospin excitations in RPA

In this Appendix we find the spectrum of isospin excitations both in the disordered and ordered phases. Above T_c , $M_n^z = 0$ and $M_n^x = M \neq 0$. It is convenient to perform a rotation in the isospace:

$$\begin{bmatrix} T_n^x \\ T_n^y \\ T_n^z \end{bmatrix} \rightarrow \begin{bmatrix} T_n'^x \\ T_n'^y \\ T_n'^z \end{bmatrix} = \begin{bmatrix} -T_n^z \\ +T_n^y \\ +T_n^x \end{bmatrix}. \quad (25)$$

In the rotated basis $\langle T_n'^z \rangle = M$ and the Hamiltonian has the form:

$$H_T = -2t_\perp \sum_{\mathbf{n}} T_n'^z + \frac{1}{2} \sum_{\mathbf{nm}} V_{\mathbf{nm}} T_n'^x T_m'^x, \quad (26)$$

We then use the equations of motion for the operators $T_n'^\pm = T_n'^x \pm iT_n'^y$:

$$\pm i\dot{T}_n'^\pm = 2t_\perp T_n'^\pm + \frac{1}{2} \sum_{\mathbf{m}} V_{\mathbf{nm}} T_n'^z (T_m'^+ + T_m'^-), \quad (27)$$

in which we substitute T_n^z by its average value, M . This approximation, equivalent to the decoupling of the Green functions containing more than two isospin operators [39, 40], gives a closed system of equations,

$$\begin{cases} \left[\omega - 2t_\perp - \frac{M}{2}V(\mathbf{q}) \right] \langle\langle T'^+ | T'^- \rangle\rangle - \frac{M}{2}V(\mathbf{q}) \langle\langle T'^- | T'^- \rangle\rangle = 2M \\ \frac{M}{2}V(\mathbf{q}) \langle\langle T'^+ | T'^- \rangle\rangle + \left[\omega + 2t_\perp + \frac{M}{2}V(\mathbf{q}) \right] \langle\langle T'^- | T'^- \rangle\rangle = 0 \end{cases}, \quad (28)$$

for the retarded Green functions $\langle\langle A|B \rangle\rangle \equiv \langle\langle A|B \rangle\rangle_{\omega, \mathbf{q}}$, defined by

$$\langle\langle A|B \rangle\rangle_{\omega, \mathbf{q}} = -i \int_0^\infty dt e^{i(\omega+i\delta)t} \sum_{\mathbf{n}} e^{-i\mathbf{q}\cdot\mathbf{x}_n} \langle[A, B]\rangle. \quad (29)$$

In this way we get:

$$\begin{cases} \langle\langle T'^+ | T'^- \rangle\rangle_{\omega, \mathbf{q}} = 2M \frac{(\omega + 2t_\perp + \frac{M}{2}V(\mathbf{q}))}{\omega^2 - E_{\mathbf{q}}^2 + i\delta \text{sign}\omega}, \\ \langle\langle T'^- | T'^- \rangle\rangle_{\omega, \mathbf{q}} = -\frac{M^2 V(\mathbf{q})}{\omega^2 - E_{\mathbf{q}}^2 + i\delta \text{sign}\omega}. \end{cases} \quad (30)$$

Furthermore,

$$\begin{cases} \langle\langle T'^- | T'^+ \rangle\rangle_{+\omega, \mathbf{q}} = \langle\langle T'^+ | T'^- \rangle\rangle_{-\omega, \mathbf{q}}, \\ \langle\langle T'^+ | T'^+ \rangle\rangle_{\omega, \mathbf{q}} = \langle\langle T'^- | T'^- \rangle\rangle_{\omega, \mathbf{q}}. \end{cases} \quad (31)$$

The Green functions have poles at (plus/minus) the energy of the isospin excitation with wave vector \mathbf{q} :

$$E_{\mathbf{q}} = \sqrt{2t_{\perp}(2t_{\perp} + MV(\mathbf{q}))}. \quad (32)$$

The band of isospin excitations has its bottom at the wave vector $\mathbf{q} = \mathbf{Q}$, where $V(\mathbf{q})$ has its minimum.

Combining Eqs.(30) and (31) we obtain:

$$\langle\langle T^z | T^z \rangle\rangle_{\omega, \mathbf{q}} = \langle\langle T'^x | T'^x \rangle\rangle = \frac{2t_{\perp}M}{(\omega^2 - E_{\mathbf{q}}^2 + i\delta\text{sign}\omega)}. \quad (33)$$

In the ordered phase below T_c we introduce on each site \mathbf{n} an angle $\phi_{\mathbf{n}}$ by

$$\begin{cases} M_{\mathbf{n}}^x = M_{\mathbf{n}} \cos \phi_{\mathbf{n}} \\ M_{\mathbf{n}}^z = M_{\mathbf{n}} \sin \phi_{\mathbf{n}} \end{cases}, \quad (34)$$

where we used the original basis. Then the first of the self-consistency equations Eq.(8) reads:

$$2t_{\perp} \sin \phi_{\mathbf{n}} + \cos \phi_{\mathbf{n}} \sum_{\mathbf{m}} V_{\mathbf{nm}} M_{\mathbf{m}} \sin \phi_{\mathbf{m}} = 0. \quad (35)$$

We now chose the basis in the isospin space, such that the z -axis is oriented along $\langle \mathbf{T}_{\mathbf{n}} \rangle$:

$$\begin{cases} T'_{\mathbf{n}}^x = \sin \phi_{\mathbf{n}} T_{\mathbf{n}}^x - \cos \phi_{\mathbf{n}} T_{\mathbf{n}}^z, \\ T'_{\mathbf{n}}^y = T_{\mathbf{n}}^y, \\ T'_{\mathbf{n}}^z = \cos \phi_{\mathbf{n}} T_{\mathbf{n}}^x + \sin \phi_{\mathbf{n}} T_{\mathbf{n}}^z. \end{cases} \quad (36)$$

Then $\langle T'_{\mathbf{n}}^z \rangle = M_{\mathbf{n}}$ and $\langle T'_{\mathbf{n}}^x \rangle = \langle T'_{\mathbf{n}}^y \rangle = 0$.

Using Eq.(35) the linearized equations of motion for T'^{\pm} can be written in the form:

$$\pm i\dot{T}'_{\mathbf{n}}^{\pm} = \frac{2t_{\perp}}{\cos \phi_{\mathbf{n}}} T'_{\mathbf{n}}^{\pm} + \frac{1}{2} M_{\mathbf{n}} \cos \phi_{\mathbf{n}} \sum_{\mathbf{m}} V_{\mathbf{nm}} \cos \phi_{\mathbf{m}} (T'_{\mathbf{m}}^{+} + T'_{\mathbf{m}}^{-}). \quad (37)$$

Both for the zigzag and the chain ordering,

$$\phi_{\mathbf{n}} = e^{i\mathbf{Q}\cdot\mathbf{x}_{\mathbf{n}}}\phi, \quad (38)$$

and $|\phi_{\mathbf{n}}| = \phi$. Then, Eq.(35) gives $M_{\mathbf{n}} = M$ and

$$M = \frac{2t_{\perp}}{\cos\phi|V(\mathbf{Q})|}, \quad (39)$$

(*cf.* Eq.(10)). Furthermore, from Eq.(37) we see that the Green functions in the ordered phase can be obtained from those above T_c by substituting $2t_{\perp}$ by $\frac{2t_{\perp}}{\cos\phi}$ and $V(\mathbf{q})$ by $V(\mathbf{q})\cos^2\phi$, *e.g.*,

$$\langle\langle T'^+|T'^- \rangle\rangle_{\omega,\mathbf{q}} = 2M \frac{\left(\omega + \frac{2t_{\perp}}{\cos\phi} + \frac{M}{2}\cos^2\phi V(\mathbf{q})\right)}{\omega^2 - E_{\mathbf{q}}^2 + i\delta\text{sign}\omega}, \quad (40)$$

where the energy of the isospin excitations is given by

$$E_{\mathbf{q}} = \frac{2t_{\perp}}{\cos\phi} \sqrt{1 - \cos^2\phi^2 \frac{V(\mathbf{q})}{V(\mathbf{Q})}}. \quad (41)$$

Since below T_c , $0 < \cos\phi < 1$, the isospin gap in the ordered phase, $\Delta = E_{\mathbf{Q}} = 2t_{\perp}\tan\phi > 0$. The dispersion relations Eq.(32) and Eq.(41) can be combined to give Eq.(15) valid both above and below T_c .

Using Eq.(35), one can check that the Green functions of T'^z and any other operator vanish. Then, $\langle\langle T^z|T^z \rangle\rangle_{\omega,\mathbf{q}} = \cos^2\phi\langle\langle T'^x|T'^x \rangle\rangle$, so that below T_c ,

$$\langle\langle T^z|T^z \rangle\rangle_{\omega,\mathbf{q}} = \frac{(2t_{\perp})^2}{|V(\mathbf{Q})|} \frac{1}{\left(\omega^2 - E_{\mathbf{q}}^2 + i\delta\text{sign}\omega\right)} \quad (42)$$